Electronic Supplementary Material (ESI) for Polymer Chemistry.

-Supporting Information-

Redox-sensitive ferrocene functionalised double cross-linked supramolecular hydrogels

Nikolai Liubimtsev[a,b], Tom Kösterke[a,b], Yunjiao Che[a], Dietmar Appelhans[a], Jens Gaitzsch[a,*], Brigitte Voit[a,b,*]

[a] Leibniz-Institut für Polymerforschung Dresden e.V., Hohe Straße 6, 01069 Dresden, Germany

[b] Technische Universität Dresden, Faculty of Chemistry and Food Chemistry, Organic Chemistry of Polymers, 01069 Dresden, Germany

Corresponding Authors
*gaitzsch@ipfdd.de
*voit@ipfdd.de

1. Table of Contents

2. Synthesis Data

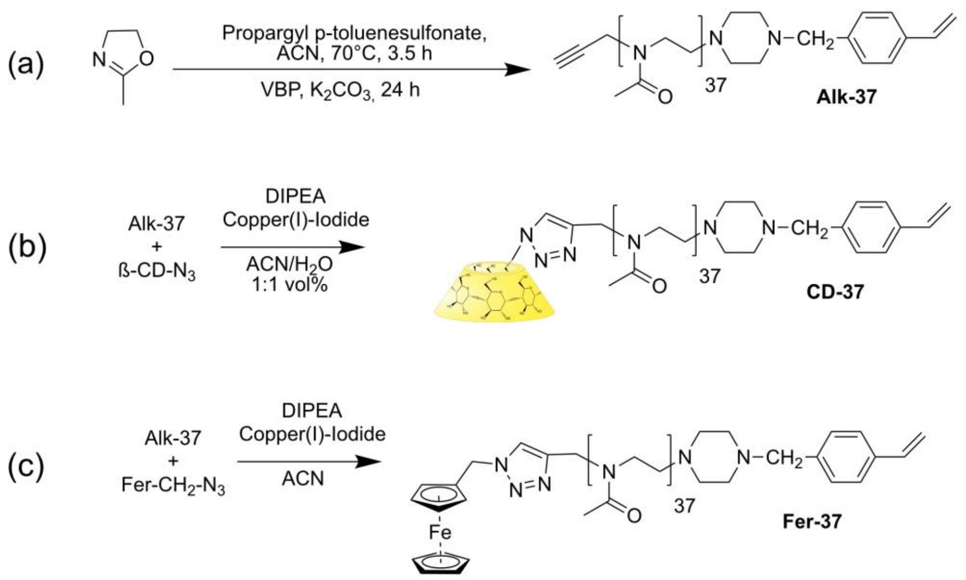

Figure S1: Overview on the polymerisation and polymer modifications of this work.

The following compiles the NMR spectra of additional substances that were not shown in the main text.

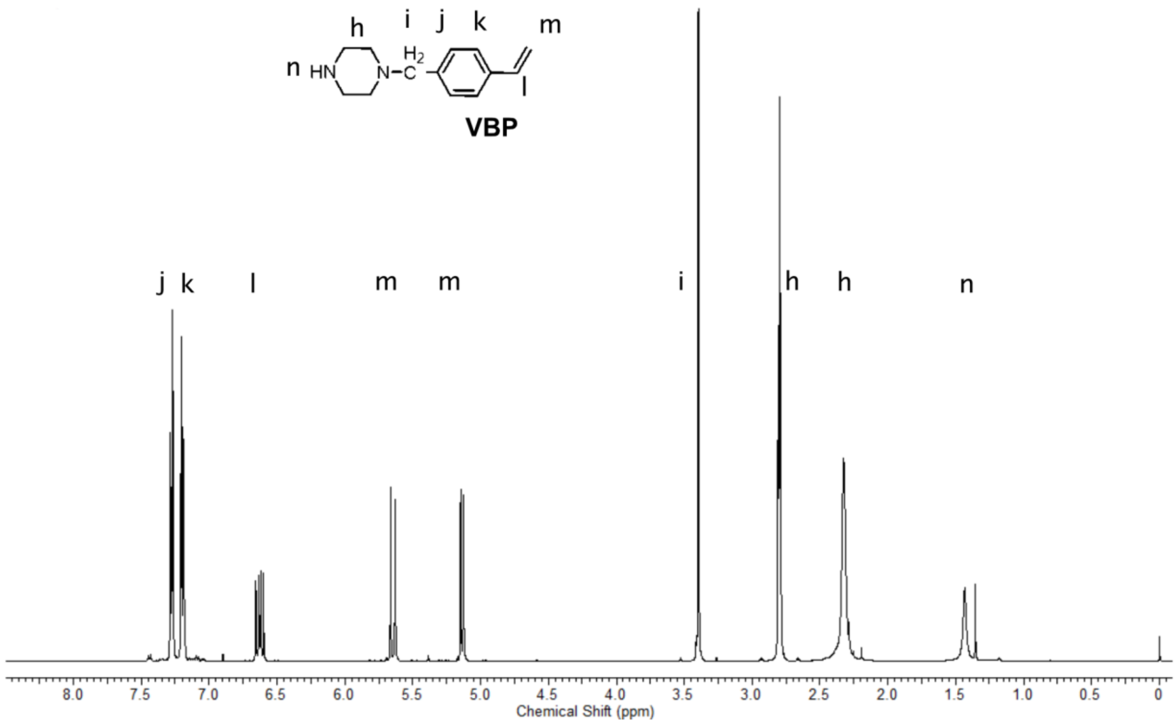

Figure S2. ^{1}H NMR spectrum of vinylating agent (VBP) recorded in $CDCl_3$.

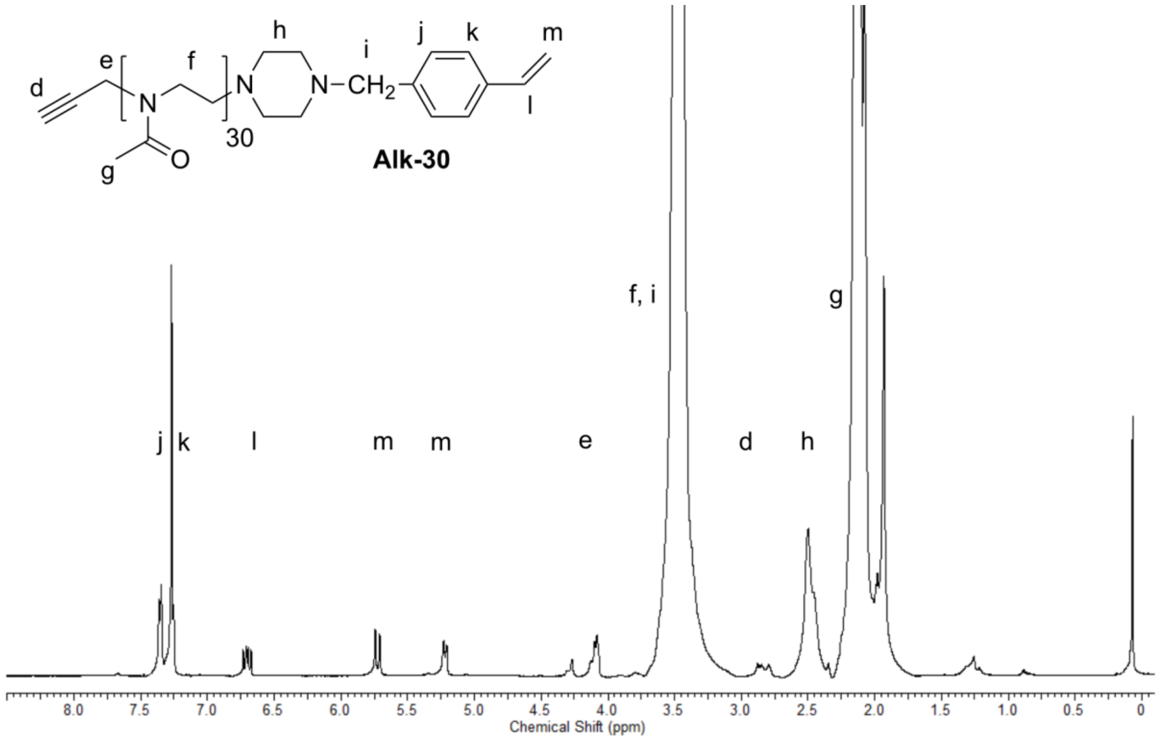

Figure S3. ^{1}H NMR spectra of alkyne-PMOXA (Alk-30) recorded in $CDCl_3$.

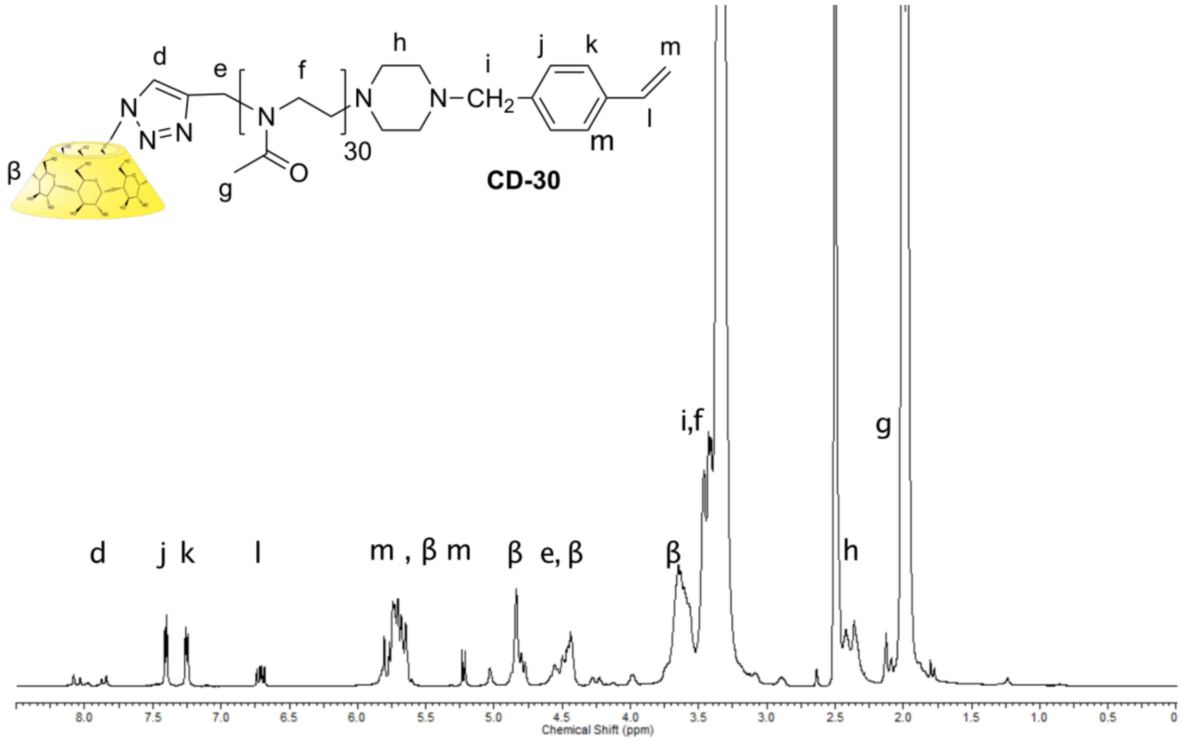

Figure S4. ^{1}H NMR spectra of CD-PMOXA (CD-30) recorded in DMSO-d_6.

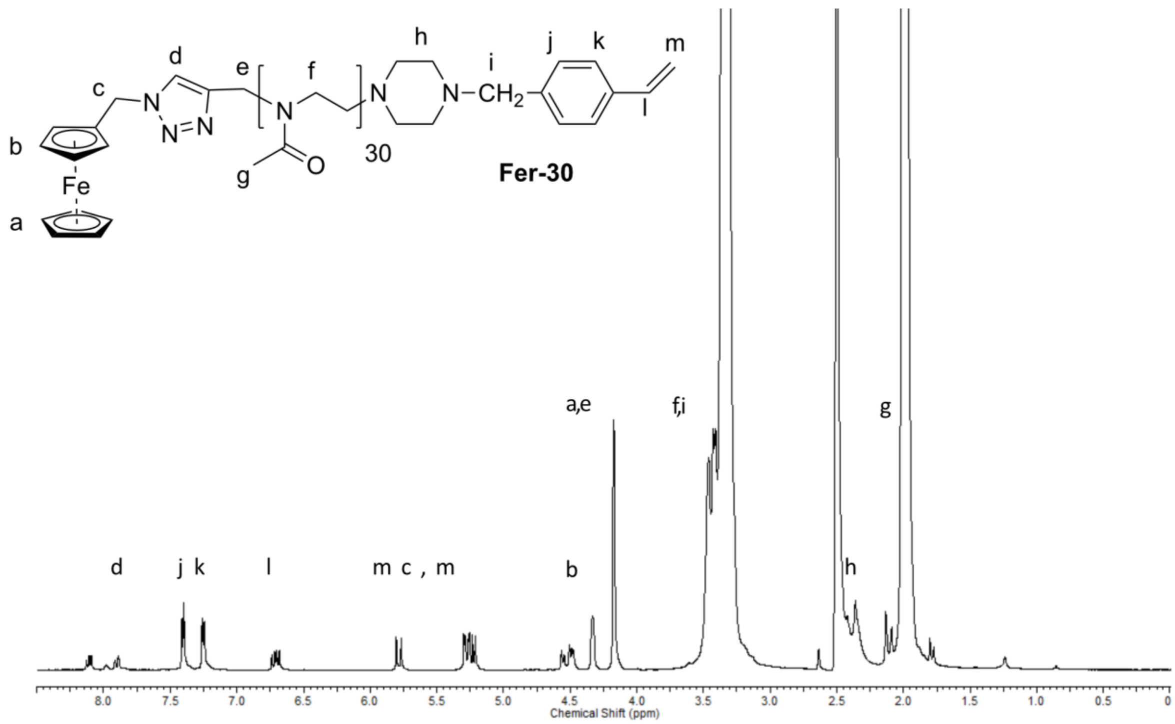

Figure S5. ^{1}H NMR spectra of ferrocene-PMOXA (Fer-30) recorded in DMSO-d_6.

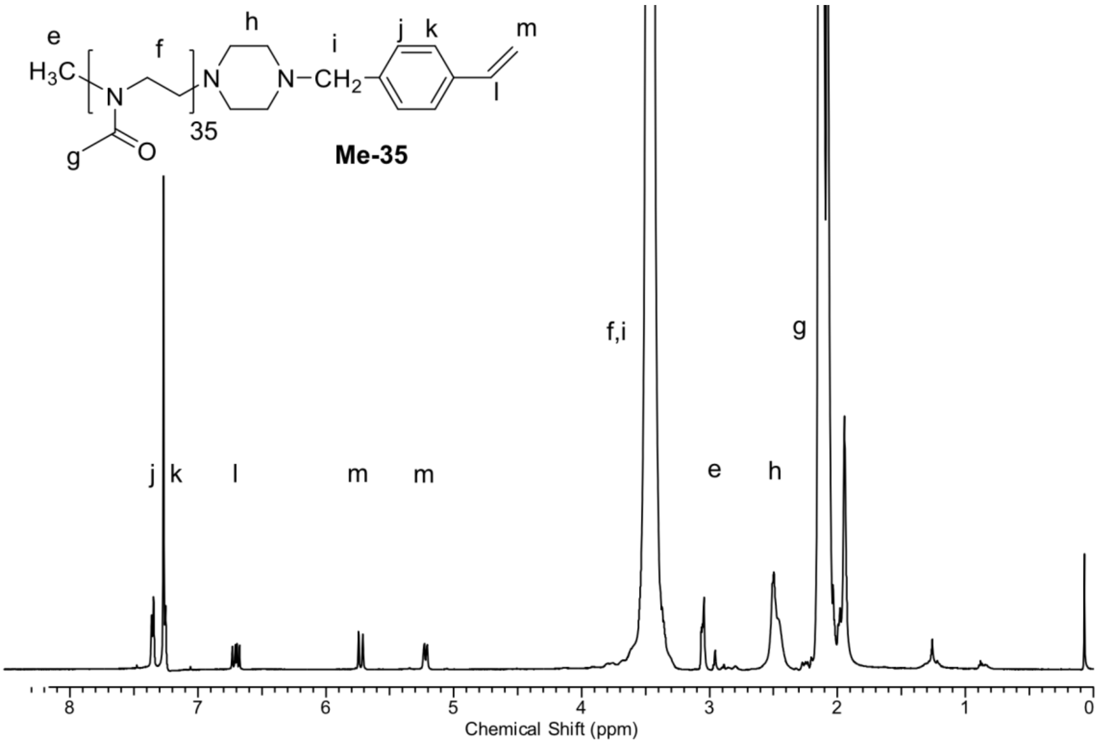

Figure S6. ^{1}H NMR spectrum of methyl-PMOXA (Me-35) recorded in $CDCl_3$.

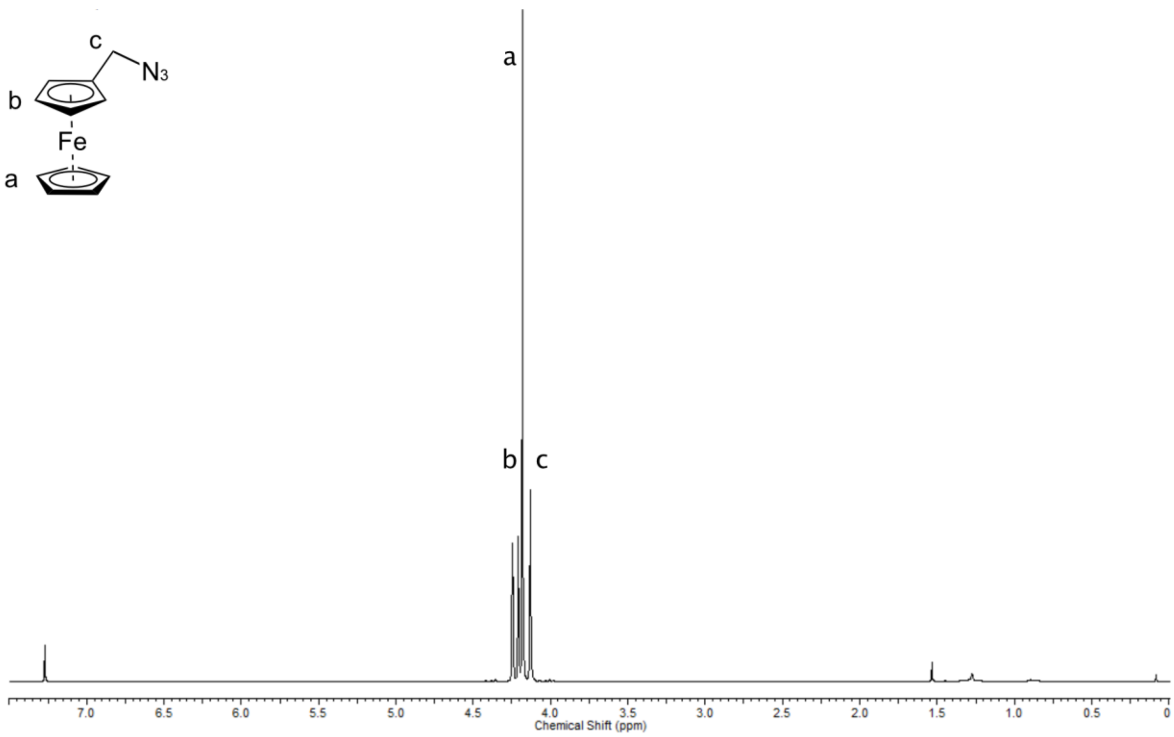

Figure S7. ^{1}H NMR spectra of azidomethylferrocene (Fer-N_3) recorded in $CDCl_3$.

3. FTIR and Raman spectra

The FTIR and Raman spectra before and after the click reaction are shown below. The loss of the azide oscillation shows the successful course of the reaction.

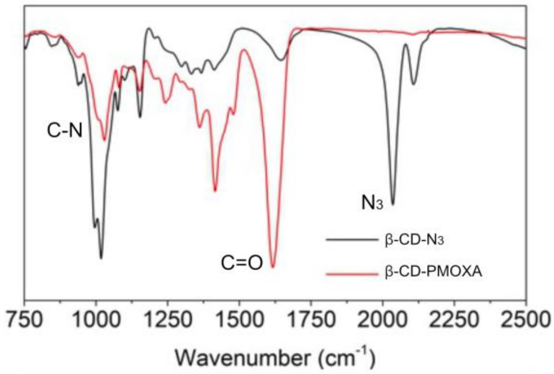

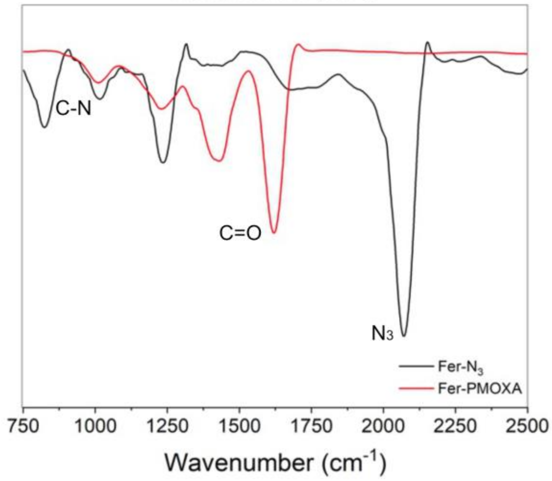

Figure S8. (a) FTIR spectra of CD-PMOXA (red line) compared with 6-monoazido-6-monodeoxy-β-cyclodextrin (black line), FTIR spectra of Fer-PMOXA (red line) compared with azidomethylferrocene (black line).

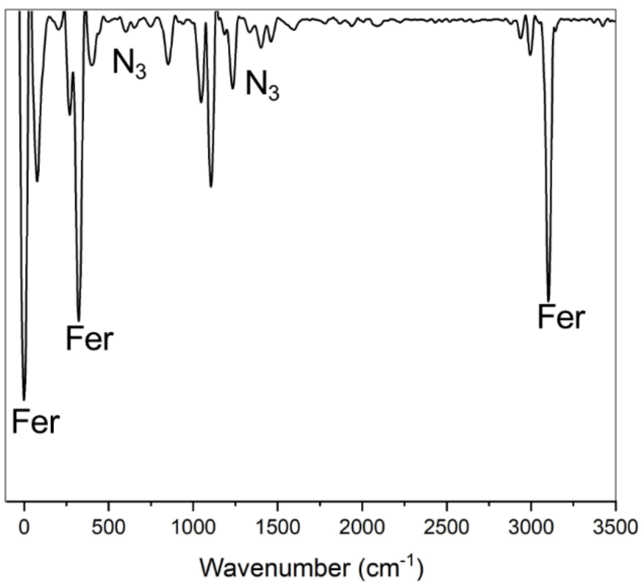

Figure S9. Raman spectra of azidomethylferrocene (Fer-N_3).

4. GPC Chromatograms

The GPC spectra of the different macromonomers are shown below. From these, the dispersities of the macromonomers were determined.

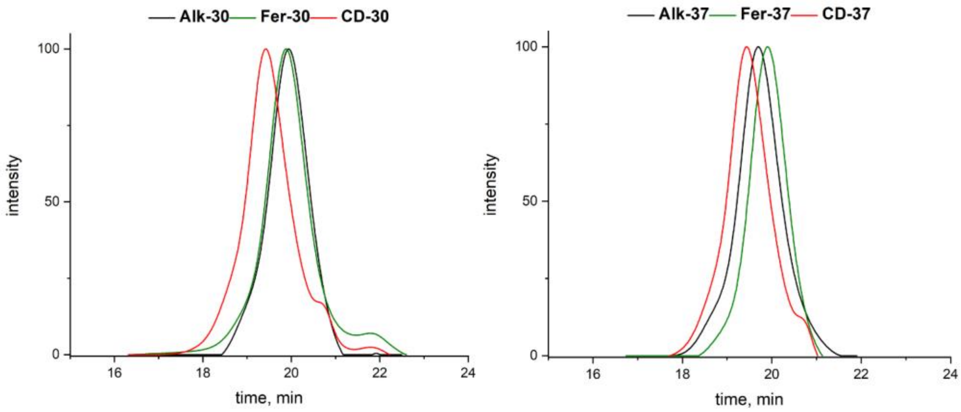

Figure S10. GPC chromatograms of Alk-30, Alk-37, CD-30, CD-37, Fer-30, Fer-37.

5. 2D NMR spectra in methanol

Below are the 2D ROESY spectra of the host-guest complex. With this method, the linkage and the breakage of the β-CD/ferrocene host-guest complex could be demonstrated and proven.

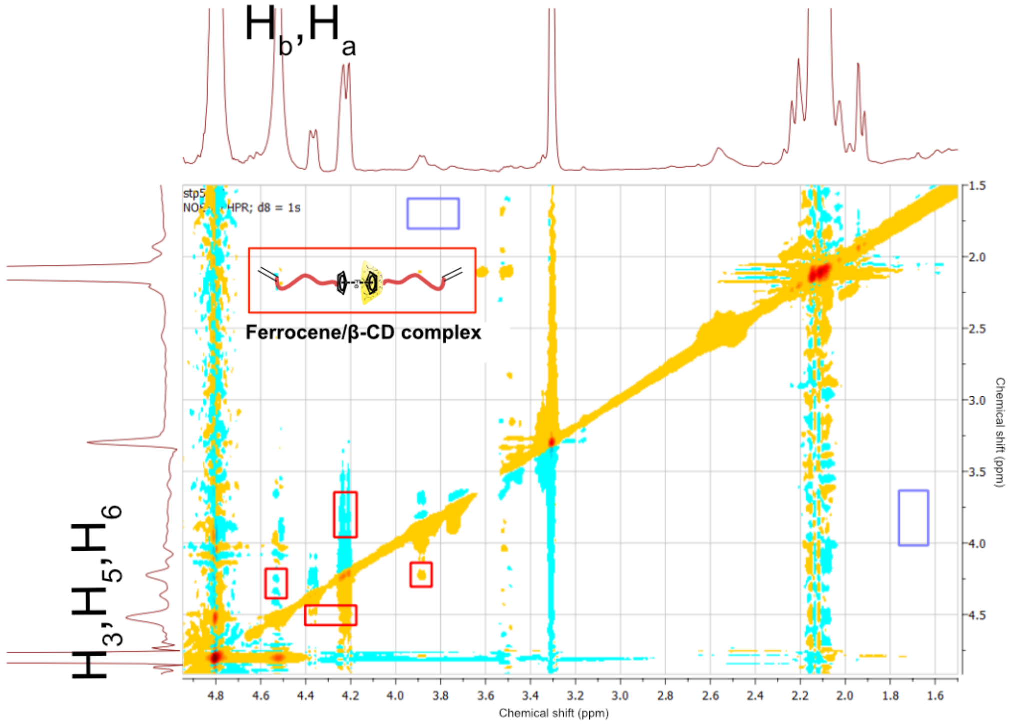

Figure S11. 2D ROESY spectrum of 1:1 molar mixture of CD-PMOXA and Fer-PMOXA (5 mmol/L) in methanol-d_4 at 30 °C for 0.994 s.

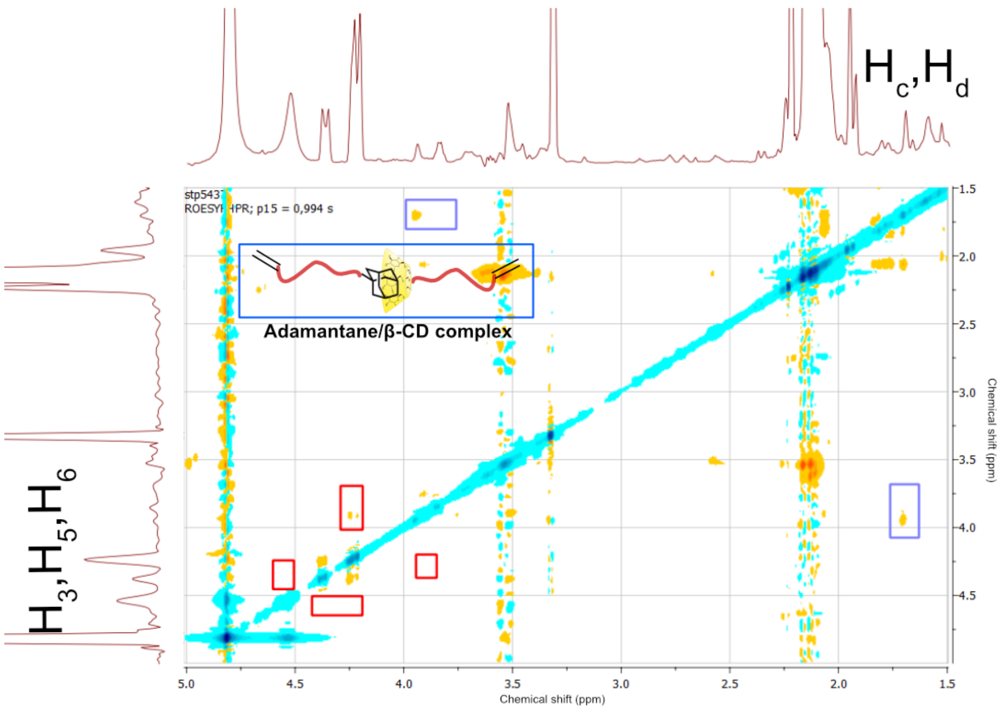

Figure S12. 2D ROESY spectrum of 1:1 molar mixture of CD-PMOXA and Fer-PMOXA (8 mmol/L) after the addition of Ada-40 in methanol-d_4 at 30 °C for 0.994 s.

6. Optimisation of the redox cycle

Before finding the optimal oxidation-reduction (i.e. swelling-deswelling) cycle, the hydrogels were already tested in a non-optimal setting (24 h cycle). This one showed a larger swelling and deswelling for the hydrogel with 1.0 mol% host-guest groups (GH-37c) compared to the hydrogel with 0.5 mol% host-guest groups (GH37a).

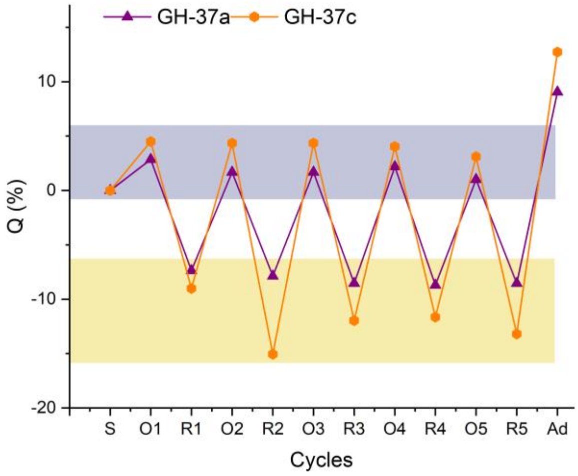

Figure S13. Oxidation and reduction for GH-37a (0.5 mol% host-guest) and GH-37c (1.0 mol% host-guest) hydrogels during a 24 h cycle that was not optimised. O1 = first oxidation, R1 = first reduction and so on.

In order to find the optimal time for the swelling and deswelling, the hydrogel with 1.0 mol% host-guest groups (GH-37c) was allowed to deswell to full equilibrium and studied using a kinetic measurement. Since full deswelling was reached after 5 hours, the whole cycle (swelling and deswelling) had to spread over 48 h in order keep a reasonable time frame.

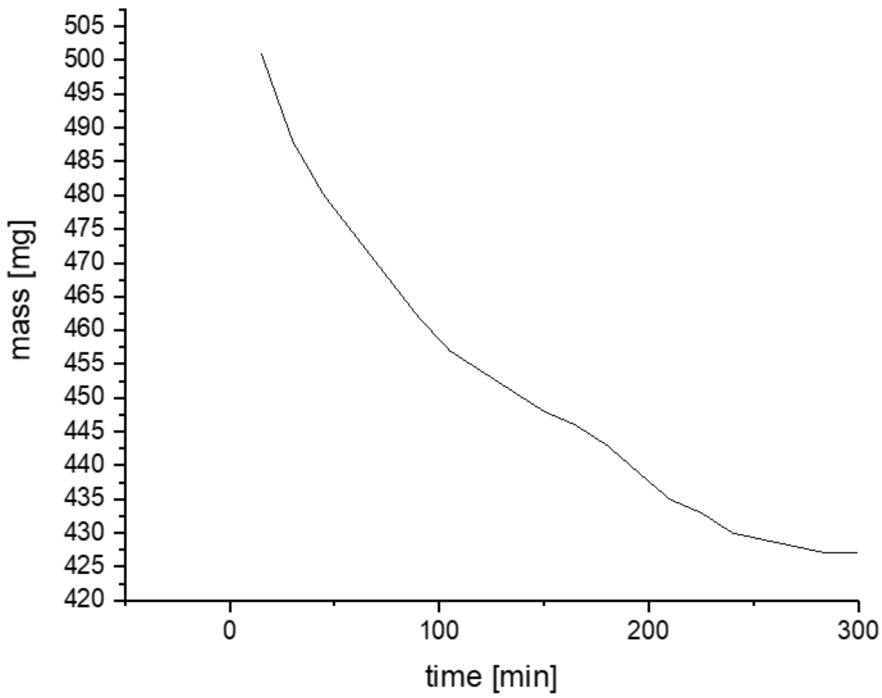

Figure S14. Kinetic study for the deswelling of GH-37c in a 10mM sodium thiosulfate solution. Full deswelling was reached after 6 h.

7. Mass and rheology data

The dynamic modulus is measured at 10 different frequencies from 1 rad/s up to 100 rad/s. The measurements points were 1; 1.58489; 2.51189; 3.98107; 6.30957; 10; 15.8489; 25.1189; 39.8107; 63.0957; 100 rad/s (Figure S15 for GH-37c). For the values noted in the tables below and hence also for Fig. 6 of the main paper, we took the average from the point 3 to 8, because the first and last two values deviated slightly from the flat region, both in the storage and in the loss modulus. The storage over loss values did not deviate greatly over the frequency sweep and can be seen on the graphic, where it belongs to the second y-axis (the one on the right).

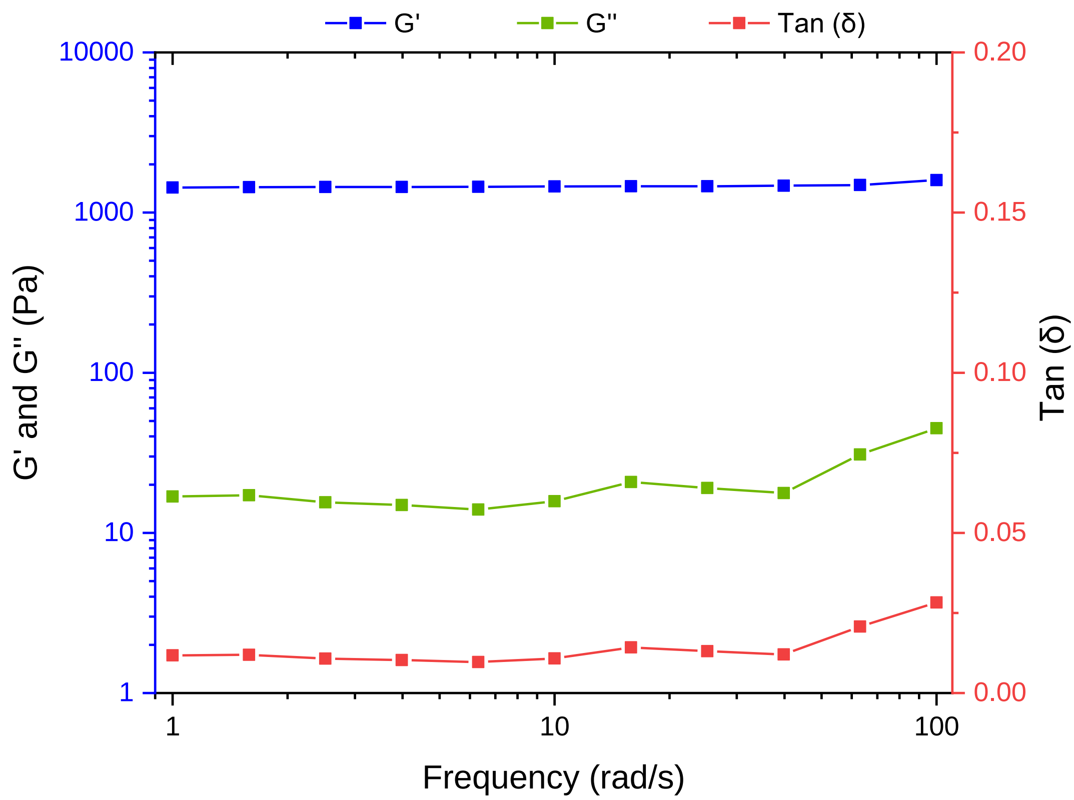

Figure S15. Dynamic measurement of the loss and storage modulus (in Pa) as well as the loss factor, exemplary shown for GH-37c.

The numerical data for Figure 6 are comprised in the following tables:

Mass of hydrogels in mg (Fig. 6a):

Cycle	GH-37a	GH-37c	GH-30a	H-PNiPAAm	GH-35Me
Start	516	538	658	339	352
O1	543	573	724	342	358
R1	466	487	569	335	351
O2	548	578	731	343	362
R2	474	492	568	345	349
O3	563	596	781	340	356
R3	471	505	549	339	345
O4	566	576	765	341	355
R4	476	496	556	336	344
O5	574	582	770	334	352
R5	477	499	571	335	347
Ad	591	606	792	338	359

Storage modulus in Pa (Fig. 6b):

Cycles	GH-37a	GH-37c	GH-30a		GH-35Me
O1	1689	1447	563		5611
R1	2168	1510	735		5654
O2	1664	1399	527		5507
R2	1925	1461	449		5635
O3	1655	1419	515		5511
R3	1848	1457	554		5568
O4	1613	1424	503		5472
R4	1854	1453	543		5572
O5	1637	1395	422		5391
R5	1873	1425	524		5646
Ad	1818	1202	421		5336